Spatial force correlations in granular shear flow. I. Numerical evidence

Gregg Lois,[1] Anaël Lemaître,[2] and Jean M. Carlson[1]

[1]*Department of Physics, University of California, Santa Barbara, California 93106, USA*
[2]*Institut Navier–LMSGC, 2 allée Képler, 77420 Champs-sur-Marne, France*

We investigate the emergence of correlations in granular shear flow. By increasing the density of a simulated granular flow, we observe a transition from a dilute regime, where interactions are dominated by binary collisions, to a dense regime characterized by large force networks and collective motions. With increasing density, interacting grains tend to form networks of simultaneous contacts due to the dissipative nature of collisions. We quantify the size of these networks by measuring two-point force correlations and find dramatic changes in the statistics of contact forces as the size of the networks increases.

I. INTRODUCTION

Granular materials exhibit a wide range of fascinating behaviors [1], but predictive theories linking the microscopic grain interactions to macroscopic properties remain a topic of much debate. Of particular interest are constitutive relations for granular flow, which are important for engineering and geophysical applications [2,3] and challenge the tenets of conventional statistical physics [4]. Because granular materials are athermal, their dynamics always occur far from equilibrium, and a proper formulation of constitutive relations relies on the construction of nonequilibrium statistical theories that must be sensitive to the interactions between grains.

Interactions in realistic granular materials arise due to grain elasticity and friction, but are complicated by various other mechanisms, including humidity [5–9], grain shapes [10–12], and fracture processes occurring within the material [13]. A great deal of theoretical and computational progress has been made using the simple approximation that grains are spherical and perfectly dry [14]. In this case a purely repulsive force arises when two grains come into contact due to the deformation of grains and friction between grains.

Understanding the nature of grain forces and dynamics, even in this relatively simple case, has proven difficult. At very low densities it can safely be assumed that only binary interactions occur, and constitutive relations can be determined by statistically tracking the repulsive force created in each interaction. This is the basis of kinetic theory, which has been successfully applied to granular flows [15,16]. However, for very large densities, it is observed that multigrain contacts always occur [17–19] and contact forces are transmitted through "force chain networks" formed by the topology of the contact network [14,21–23]. For these high densities the forces between contacting grains still arise from grain deformation and friction, but the extent of the interactions is not localized and depends on properties of the force chain networks.

The presence of force chain networks calls into question theories that assume localized interactions and has inspired new models based on properties of the force chains [24–30]. However, although force networks can be visualized, it has proven difficult to measure quantitative correlations between contact forces [31–34]. This led to the speculation that force

chain networks are simply a perceived correlation, until recently, when spatial correlations were measured between the *averaged* contact forces in a quasistatic experimental shear flow at high density [23].

This discovery raises important questions about the proper assumptions to make when constructing theories of granular materials. For very dilute systems only binary collisions occur, and force chain networks do not play a role; for very dense systems force networks are the dominant microscopic interaction. In order to understand the origin of macroscopic properties in granular flows, it is necessary to pinpoint exactly how and when correlations appear.

In this paper we measure spatial correlations of the *total* force on grains undergoing shear deformation. This measurement defines a characteristic length scale ξ quantifying the size of force networks arising from clusters of simultaneously contacting grains. We find that ξ grows with packing fraction, diverges at a finite packing fraction, and has measurable effects on the contact forces between grains. The correlation measurement also provides a natural boundary between dilute flows where only binary collisions occur and dense flows where force networks emerge.

We begin in Sec. II by briefly outlining the phenomenology of granular shear flow to define the exact regime we will be studying. In Sec. III we discuss the numerical algorithm used to simulate shear flow. In Sec. IV we introduce the spatial force correlation measurement, which provides a natural definition for a correlation length, and in Sec. V we show how the size of the correlation length affects contact forces between grains.

II. GRANULAR SHEAR FLOW: BASIC CONSIDERATIONS

If no external force is applied to a dry granular material in the absence of gravity, it quickly loses all its kinetic energy in dissipative collisions, and each grain comes to rest. If this occurs for a dilute system there are no residual contacts between any grains and the total energy is zero. However, for granular materials with larger densities, there are contacts between grains in the relaxed state and a nonzero residual energy remains due to grain deformation and friction.

If a shear stress is then applied to the system, motion occurs only if the stress is large enough to overcome the

energy stored in the contacts. The minimum stress needed to initiate motion is called the yield stress; it is zero below a critical packing fraction ν_c and is an increasing function of packing fraction above ν_c [35–37].

For granular shear flows with $\nu > \nu_c$, previous research has demonstrated that the stiffness of the grains plays an important role at all values of the shear rate [38]. This is because grains are not able to rearrange to a configuration where no contacts exist and the system moves between different configurations where the grains are always deformed. Shear flows with $\nu > \nu_c$ are characterized by slowly moving quasistatic flows [39,40], where force balance is upheld at all times, and jamming [35–37], where motion ceases for stresses below the yield stress.

Conversely, for granular shear flows with $\nu < \nu_c$, it has been demonstrated that the stiffness of the grains can always be taken large enough so that it plays no role in the dynamics [38,41–43]. This is because grains are always able to rearrange to find free volume, and the system moves between different configurations with minute grain deformation. In this regime inertial terms are dominant, and an invariance in Newton's equations [44]. proves that the dynamics are controlled exclusively by the shear rate $\dot{\gamma}$ [45]. For these inertial flows the stress tensor is proportional to $\dot{\gamma}^2$, which is referred to as Bagnold's scaling and has been observed in experiments [46] and simulations [41,42,45].

In this paper we consider only inertial flows of granular materials with $\nu < \nu_c$, in the limit of infinite stiffness. This allows us to investigate a wide range of packing fractions, from zero to ν_c, and explore how correlations between grains naturally emerge in this range. In particular, we measure spatial force correlations and observe that they decay exponentially with a characteristic length scale ξ. By measuring distributions of contact forces, we demonstrate that only binary collisions are relevant for small ξ, and simultaneous contacts have quantitative effects on contact forces for large ξ. This allows us to define an important packing fraction ν_{bc}, where the crossover occurs between binary collisions and force networks. This crossover is accompanied by a signature in the contact force probability distribution function that has been observed previously in experiments on hopper flow [47].

The transition at ν_{bc} is purely dynamical and would not occur if $\dot{\gamma}=0$. We find that the value of ν_{bc} depends on the amount of energy dissipated at each contact, but it is always the case that ν_{bc} is strictly less than ν_c. This separates the inertial regime into a dilute inertial regime, where only binary collisions are relevant, and a dense inertial regime, where clusters of contacting grains form into complex force networks. The network transition at ν_{bc} arises due to steric exclusion and is independent of the roughness of the grains. A schematic of the different regimes of granular shear flow is displayed in Fig. 1. Here we focus on flows with $\nu < \nu_c$ in order to establish the existence and importance of ν_{bc}.

III. SIMULATIONS

We perform simulations of inertial granular shear flow in two dimensions using the contact dynamics (CD) algorithm. The CD algorithm was developed to model the dynamics of
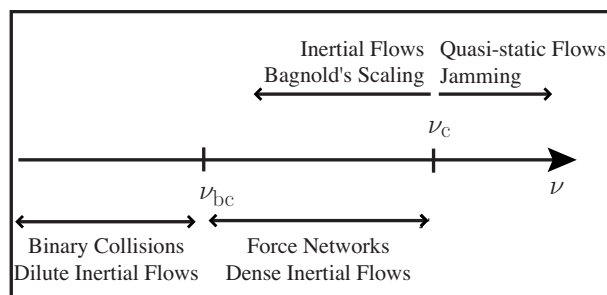

FIG. 1. Schematic of the regimes of granular shear flow. Here we explore inertial flows with $\nu < \nu_c$ and show that there is a network transition at ν_{bc} where force chain networks begin to form and affect the dynamics.

dense collections of rigid grains [48–53] and can include the effects of long-lasting, simultaneous contacts between groups of grains. It is a fully dynamical and athermal algorithm, with the motion of each grain determined at every time step by integrating Newton's equations.

To carry out the integration, the algorithm provides values for the forces between each pair of contacting grains. In dry granular materials, contact forces arise due to deformation of the grains upon contact and friction between grains. The CD algorithm considers the rigid limit in a self-consistent way, where forces take on the precise value necessary to prevent deformation, uphold Coulomb friction, and adhere to Newton's equations [48–51]. If we use $\hat{\boldsymbol{\sigma}}^{ij}$ to denote the unit vector connecting the centers of two contacting grains labeled i and j, then the deformation produces a normal force in the direction of $\hat{\boldsymbol{\sigma}}^{ij}$, and the interplay of friction and deformation produces a tangential force perpendicular to $\hat{\boldsymbol{\sigma}}^{ij}$. These contact forces are dissipative and depend sensitively on the velocities of the colliding grains [54].

The CD algorithm determines the forces arising from grain deformation by assuming that grains are infinitely rigid and setting constraints on the total energy dissipated in each contact. For two grains in contact that are approaching with a relative velocity $\mathbf{v}'^{ij}$, the algorithm determines a contact force such that the relative velocity in the next time step $\mathbf{v}^{ij}$ is given by

$$\mathbf{v}^{ij} \cdot \hat{\boldsymbol{\sigma}}^{ij} = -e\mathbf{v}'^{ij} \cdot \hat{\boldsymbol{\sigma}}^{ij}, \quad \mathbf{v}^{ij} \times \hat{\boldsymbol{\sigma}}^{ij} = e_t \mathbf{v}'^{ij} \times \hat{\boldsymbol{\sigma}}^{ij}. \quad (1)$$

In this way, the relative velocities are altered by restitution coefficients in the normal (e) and tangential directions (e_t). This procedure ensures that the momentum transferred between grains with nonzero relative velocities is at least that which is supposed to arise from collision. Friction is included by assuming that the grains have a coefficient of friction μ. If the ratio of the tangential to the normal force exceeds μ, then the grains are allowed to slip with a tangential force equal to μ times the normal force. Using these dynamical constraints, contact forces can be determined at each time step.

It is important to mention one subtlety of the algorithm: because a constant time step is utilized, many contacts can

(and do) occur in each time step. In this case, all contacts are assumed to occur simultaneously and the dynamical rule in Eq. (1), along with the friction constraint, is applied to each contact. This leads to a set of coupled algebraic equations for each group of contacting grains that is solved using an iterative method. Therefore, the value of a specific contact force depends not only on properties of the contacting grains, but also on the properties of other grains in the connected cluster. Physically this corresponds to the effects of contact forces being propagated through a network of grains, much faster than contacts are created and/or destroyed. The CD algorithm explores the limit of infinitely rigid grains by assuming that the propagation occurs instantaneously.

The limit of infinitely rigid grains has also been explored in other simulations [38,41–43]. In one study [38], Campbell simulated soft spheres with a rigidity k in shear flow at constant volume. He found that, for any packing fraction below a critical value ν_c, k can be taken large enough so that no macroscopic variables depend on its value. This study, along with others [41–43], establishes the validity of the "hard-sphere" limit in granular shear flow.

Shear flows of hard-sphere granular materials always occur in the inertial regime [44,45]. Because the stiffness of the grains does not play a role, the interactions between grains are mediated by dimensionless quantities, as in Eq. (1), and the only time scale is set by the value of the external shear rate $\dot{\gamma}$. Therefore, by dimensional analysis, it must be the case that the pressure and the shear stress are proportional to $\dot{\gamma}^2$. This is Bagnold's scaling [46], which is a central characteristic of granular flows in the inertial regime. Since hard-sphere granular flows must always occur in the inertial regime, our simulations are constrained to lie below the jamming transition at ν_c and always have zero yield stress. However, we can explore granular flows arbitrarily close to ν_c, and we have conducted simulations up to a packing fraction of 0.84.

The value of ν_c in our system is ultimately determined by the distribution of grain sizes. In the simulations presented here we use a polydisperse collection of circular grains in two dimensions. The grain diameters are chosen randomly from a flat distribution with minimum and maximum diameters given by $\sigma\pm\Delta$, with $\sigma=1.4$ and $\Delta=0.26\sigma$. We have found that this amount of polydispersity restricts crystallization. We estimate that the value of ν_c for this grain polydispersity, given the shearing algorithm, is between 0.84 and 0.85.

Finally, we comment on the shearing algorithm. We use a numerical procedure to create a simple shear flow without any boundaries. This is done using the Lees-Edwards boundary conditions [55] along with the so-called Sllod (so named because of its close relationship to the Dolls tensor algorithm) [56] equations of motion to initiate shear flow immediately. We discuss these standard procedures at length in an earlier paper [45]. For our purposes here, it suffices to state that this procedure produces a translationally invariant simple shear flow with linear velocity profile. There are no other gradients in the system, and the stress tensor, granular temperature, and packing fraction are all constant. Although this is an idealized simulation, we have shown that the resulting rheology is identical to the rheology found in steady
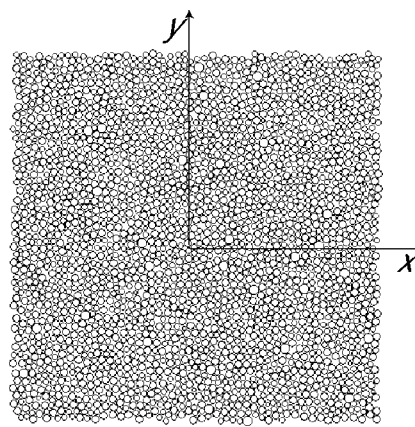

FIG. 2. Snapshot of a granular simple shear flow. Each grain has an average velocity in the x direction given by $\dot{\gamma}y$, where $\dot{\gamma}$ is the shear rate. The center of the cell is defined as $x=y=0$.

state incline flow, far from the boundaries [45]. A screenshot of our simple shear flow simulation is shown in Fig. 2.

IV. FORCE CORRELATIONS

In this section we present the central measurement of the paper. We investigate spatial force-force correlations in steady state shear flows through the measurement of the two-point correlation function

$$C(\ell) = \frac{\sum_{i=1}^{N} \sum_{j=1}^{i-1} \mathbf{F}^i \cdot \mathbf{F}^j \delta(\mathbf{r}^i - \mathbf{r}^j - \ell)}{\sum_{i=1}^{N} \mathbf{F}^i \cdot \mathbf{F}^i}. \qquad (2)$$

In this equation, $\mathbf{F}^i$ is the total vector force (sum of contact forces) experienced by grain i at position $\mathbf{r}^i$ and the sums are taken over all grains that have at least one contact. The distance ℓ ranges over the entire system size and is not limited to grains in direct contact. We take the average value of $C(\ell)$ over at least 5000 time steps in steady state shear flow. A nonzero value of $C(\ell)$ reveals that, on the average, two grains separated by a distance ℓ have forces that are correlated.

For perfectly rigid granular materials, where there is only a repulsive interaction between grains at contact, $C(\ell)$ gives a quantitative measurement of the average effect of force chains of length ℓ in the material. A nonzero value of the correlation indicates that two grains at distance ℓ are connected through a cluster of simultaneously contacting grains and the force from one grain is being transmitted through the network to the other grain. It thereby establishes that simultaneous contacts exist and that forces propagate through networks. Positive values of the correlation correspond to situations where the total forces on each grain tend to be aligned.

Because we make the measurement of $C(\ell)$ while the material is in steady state shear flow, the correlations do not reveal the presence of static structure. Instead, because contacts between grains are being created and destroyed by the
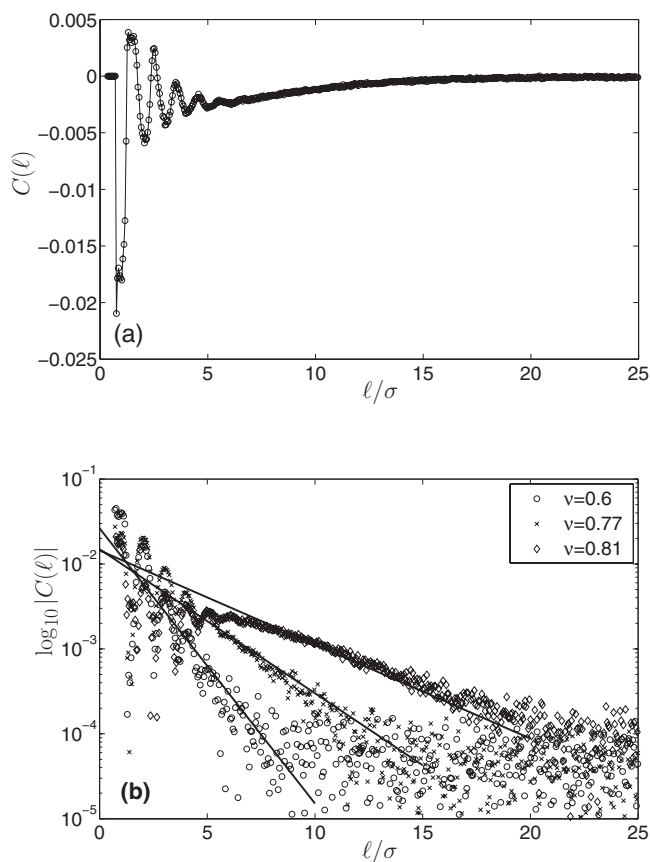
FIG. 3. (a) The force correlation function $C(\ell)$ for $e=0.25$ and $\nu=0.81$, where ℓ is the distance between grains and σ is the average grain diameter. (b) Logarithm of the magnitude, $\log_{10}|C(\ell)|$, for packing fractions of $\nu=0.6$, 0.77, and 0.81, illustrating the exponential decay of the correlations. The lines correspond to the function $e^{-\ell/\xi}$, where ξ is determined from Eq. (3) and reported in Fig. 4.

overall flow, the correlation function gives information on the average size of dynamic structures that are fluctuating in both space and time.

We will demonstrate that the correlation function depends on the vector distance $\boldsymbol{\ell}=\ell\hat{\ell}$ between pairs of grains, and that it decays exponentially with ℓ. In the following sections, we first investigate the dependence of $C(\ell)$ on the magnitude of $\boldsymbol{\ell}$, thereby defining an isotropic correlation length ξ. Then we investigate the full dependence of $C(\ell)$ and obtain the full functional form of $\xi(\theta)$, which depends on the angle θ between pairs of grains.

A. Measurements of $C(\ell)$ and the length scale ξ

We begin by measuring the isotropic part of the correlation $C(\ell)$ by averaging $C(\ell)$ over all directions $\hat{\ell}$. In Fig. 3 we plot this directionally averaged correlation function $C(\ell)$ for a frictionless material with $e=0.25$.

The logarithm of the magnitude of the correlation function, $\log_{10}|C(\ell)|$, is also plotted in Fig. 3. From these plots we observe that the magnitude decreases exponentially, although the decay is complicated by an oscillating function that accounts for the sign of $C(\ell)$. The form of this oscil-
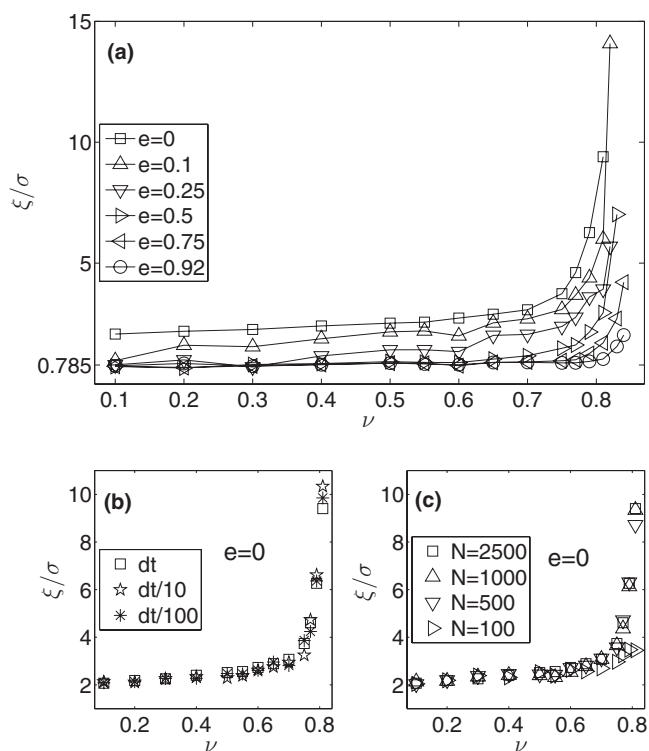

FIG. 4. (a) Length scale ξ for frictionless granular shear flows, normalized by the average radius σ, plotted for a wide range of packing fraction ν and restitution e. The value of ξ increases rapidly for large packing fraction and asymptotes to $\xi_{\mathrm{el}}/\sigma \equiv 0.785 \pm 0.022$ for small packing fraction. (b) Data for $e=0$ and multiple values of the time step. Here dt corresponds to the time step we use in this paper, which is smaller for larger packing fractions. The value of ξ does not depend on the time step. (c) Data for $e=0$ and multiple values of the particle number N. We use $N \geq 2500$ for the data in this paper. Finite size effects can be seen for $\{N=100, \nu>0.6\}$ and $\{N=500, \nu>0.8\}$. There is a large-N limit where ξ/σ is independent of system size.

lating function is not universal and depends on the exact values of the density and restitution. Nevertheless, as a first approximation, we express the correlation function as $C(\ell) \sim \exp(-\ell/\xi)$, which introduces a length scale ξ that quantifies the large-ℓ behavior of the correlations. The data in Fig. 3 illustrate that this length scale increases with packing fraction.

We find that the value of ξ is well approximated by its expectation value

$$\xi = \frac{\displaystyle\int_0^\infty d\ell \, \ell C(\ell)}{\displaystyle\int_0^\infty d\ell \, C(\ell)}. \qquad (3)$$

In Fig. 3 we plot $\exp(-\ell/\xi)$, where ξ is determined for each density from Eq. (3), and we observe excellent agreement with the measured exponential decays of $C(\ell)$.

In Fig. 4 we plot measurements of ξ, determined from Eq. (3), for all of the frictionless granular flows we have simu-

lated. The value of ξ quantifies the average extent of force chains in the system and is an increasing function of density for each value of restitution. Higher values of restitution have lower values of ξ. This is consistent with the picture of dynamic force networks forming as the material is sheared due to energy dissipation upon contact. Indeed, in the limit of $e \to 1$, the data in Fig. 4 suggest that no correlations exist.

The formation of correlations in sheared granular materials is likely caused by inelastic collapse [57]. Collapsing grains contact increasingly often, allowing a single grain to have multiple contacts, even in the limit of perfectly rigid grains [60]. While previous studies [57–59] have focused on the initial stages of inelastic collapse, concluding that multiple collisions become important as the packing fraction is increased, here we study the properties of the fully collapsed clusters in the steady state. One of the major differences is that the correlation length we measure does not depend on system size, whereas the onset of inelastic collapse shows a strong system size dependence for all sizes investigated [57]. This makes it difficult to directly compare the onsets of inelastic collapse and force correlations. However, for all the systems investigated here, if we compare the packing fraction $\nu_{bc}(e)$ at which correlations first develop to the onset $\nu^*(e)$ of inelastic collapse for a given system size (using the values given in Ref. [57]), it is always the case that $\nu_{bc}(e) > \nu^*(e)$. This means that, as we increase the density for a given restitution coefficient and system size, inelastic collapse always occurs *before* force correlations develop.

For large values of the packing fraction, the value of ξ increases rapidly. The maximum packing fraction we simulate is $\nu_{max} = 0.84$, but we were not able to determine the value of ξ at ν_{max} for all values of restitution. This is because, for very large packing fractions and small restitution coefficients, the correlation function we measure from Eq. (2) does not decay to zero by the maximum length $\ell \approx 50$ that we can access in our largest simulations of 100×100 grains. Since this implies that correlations extend beyond the system size, we do not include these data.

For large values of the packing fraction, we conduct simulations in increments of $\Delta \nu = 0.01$. When $e \leq 0.5$, we reach a packing fraction where, if we increase the packing fraction by 0.01, ξ is too large to be measured. The rapid growth of the correlations at high packing fraction suggests that ξ is diverging. We include a plot of ξ as a function of $\nu_c - \nu$ in Fig. 5. We approximate $\nu_c = 0.845 \pm 0.005$, which is the source of the horizontal error bars. As ν approaches its maximum value ν_c, the value of ξ increases. Limits on the maximum system size preclude us from making definite statements about the functional form of the divergence.

For small values of packing fraction and large restitution coefficients, ξ approaches a limiting value of $\xi_{el} = (0.785 \pm 0.022)\sigma$, which we have determined by averaging the values of ξ for $e = 0.92$ and $\nu \leq 0.4$. This corresponds to the smallest correlation possible, which arises when the only relevant interactions are binary collisions between grains. For these small packing fractions, the sign of $C(\ell)$ is exclusively negative and the exponential decay is not observed. Indeed, in the limited simulations we have conducted with a monodisperse collection at very low packing fraction, we
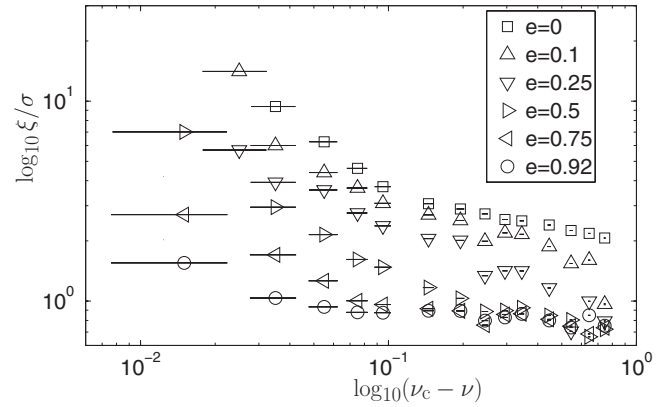

FIG. 5. Length scale ξ, normalized by the average radius σ, as a function of $\nu_c - \nu$ for many restitution coefficients e. We estimate that the jamming transition occurs at $\nu_c = 0.845 \pm 0.005$ for the grain polydispersity used here.

observe that $C(\ell)$ is zero for all values of ℓ except $\ell = \sigma$. In the case of a polydisperse collection of grains, the form of $C(\ell)$ for dilute flows depends on the relative probabilities to have binary interactions between grains of different sizes, and exponential decay is not observed since the correlation function equals zero for all values of ℓ larger than the maximum grain diameter. Even though exponential decay is not observed in the limiting case of binary collisions between grains, Eq. (3) still provides a useful measure of correlation length that matches the exponential decay at higher densities.

The limiting value of 0.785 is related to the probability to have a binary collision between grains of different diameters and is equal to the correlation length that would be expected in a perfectly elastic system where $e = 1$ and no energy is dissipated upon interactions between grains. Thus we denote the limiting value as ξ_{el} and expect that its numerical value is related to the distribution of grain sizes. We have conducted a limited number of simulations to determine the behavior of ξ_{el} for different grain distributions, and the results are plotted in Fig. 6. Each grain distribution we consider is a flat distribution with minimum and maximum grain diameters given by $\sigma \pm \Delta$. As expected, $\xi_{el}/\sigma = 1$ for $\Delta = 0$. For large values of Δ, ξ_{el} depends linearly on Δ since the largest grains set the correlations. The grain distribution we consider in this paper corresponds to $\Delta = 0.26\sigma$ and is designated by a solid data point. Although this grain distribution happens to occur close to the minimum, this is not relevant to the arguments in this paper. We present the data in Fig. 6 to better understand the origin of ξ_{el}, and in particular why it differs from unity. We will argue that the ratio ξ/ξ_{el} signals the transition between different regimes of shear flow, and it asymptotes to 1 for small packing by definition.

The data we have presented for frictionless grains can also be extended to situations where $\mu > 0$. Adding friction introduces a nonzero tangential force at each contact that tends to increase geometrical frustration. Measurements of ξ for frictional systems are plotted in Fig. 7 for $e = 0$ and three friction coefficients μ. We see that the value of ξ diverges at smaller ν for systems with friction. This is to be expected, since the additional constraints associated with tangential
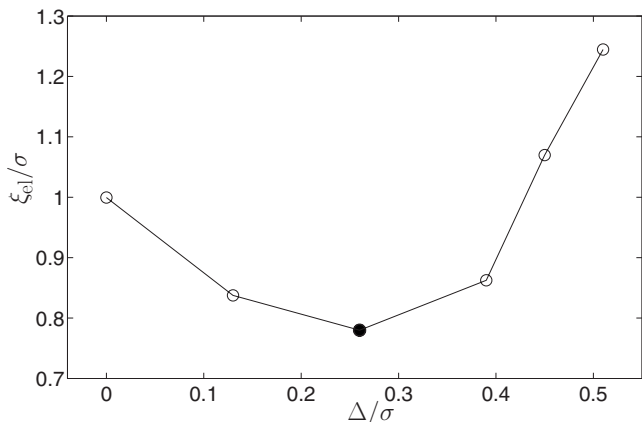
FIG. 6. Equilibrium correlation length ξ_{el} as a function of the grain distribution of the system. We consider flat distributions with minimum and maximum grain diameters given by $\sigma \pm \Delta$. The distribution considered in this paper is indicated by a solid circle.

forces can only increase the correlations. Interestingly, the value of ξ for different friction coefficients is nearly identical for $\xi < 2.5\sigma$. This is because clusters of simultaneously contacting grains must exist before the effects of friction alter the dynamics and correlations. We therefore expect that the initial emergence of correlation at ν_{bc} is not sensitive to changes in friction coefficient μ and can be understood by studying frictionless materials.

B. Connection to jamming

The data in Figs. 4 and 7 suggest that ξ diverges at a finite packing fraction ν_c that depends on the friction coefficient and possibly the restitution coefficient. This divergence is related to the jamming transition [61] in granular materials, where the shear modulus becomes nonzero and the system is able to sustain a shear stress without yielding. In order to make the transition from a flowing state to a jammed state, it is necessary that a correlation length approach the size of the system, and diverge in the thermodynamic limit. This is be-
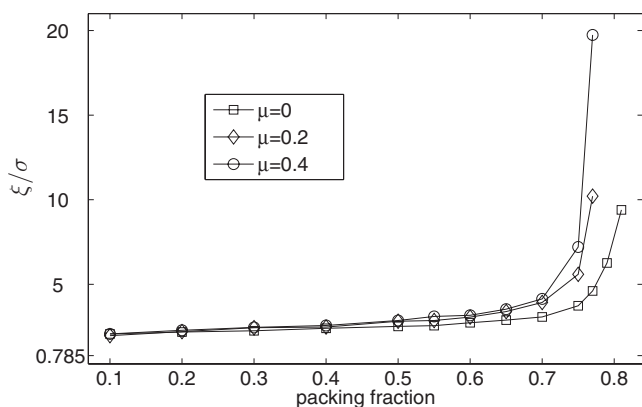

FIG. 7. Length scale ξ, normalized by average diameter σ, for granular shear flows with friction coefficient μ and $e=0$. Larger values of μ correspond to larger ξ. The value of ξ/σ is always larger than $\xi_{el}/\sigma = 0.785$.
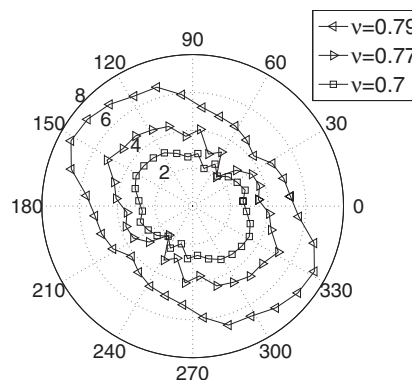

FIG. 8. Angular dependence of the length scale $\xi(\theta)$ for a frictionless shear flow with $e=0$ and three different packing fractions ν. The length scale is greatest along the compressional axis of the shear flow.

cause force chains must percolate from the upper to the lower shearing wall in order to counteract the applied shearing force. The correlation length ξ quantifies the notion of force chains, and we expect that the observed divergence of ξ is a necessary condition for jamming.

However, there is no guarantee that the divergence of ξ is also a sufficient condition for jamming, since it is possible that force chains percolate long before the system jams. Nevertheless, both theories [62,63] and simulations [35–37] have found that percolation and jamming occur simultaneously, which suggests that a granular system jams if, and only if, ξ diverges. If this holds, our data suggest that the jamming transition occurs at lower packing fraction as the friction between grains increases.

For granular shear flows near jamming, spatial correlations between grain velocities have been discussed theoretically [64] and measured in experiments [65] and simulations [66]. While these correlations are different from the force correlations measured here, they may have a similar origin. In this study we consider perfectly rigid grains where forces are transmitted instantaneously through networks, and equal time forces thereby exhibit correlations. For grains with a finite rigidity, the forces take a small amount of time to propagate through the networks and might be best studied via velocity correlations at different waiting times [66]. While a connection between these correlations is likely, it remains to be quantified.

C. Anisotropy in the angular dependence of ξ

We have also conducted measurements of the full directional dependence of $C(\ell)$. In this case, we observe that the decay of the correlations can still be described by an exponential, but the value of the correlation length depends on the orientation $\hat{\ell}$. In two dimensions this orientation can be quantified by the angle θ between ℓ and the x axis. In Fig. 8 we plot the angular dependence of ξ for frictionless flows with $e=0$ and three different packing fractions. These plots reveal that ξ is not isotropic and the correlation between a pair of grains depends on their orientation. For a simple shear flow, correlations are created along the compressional
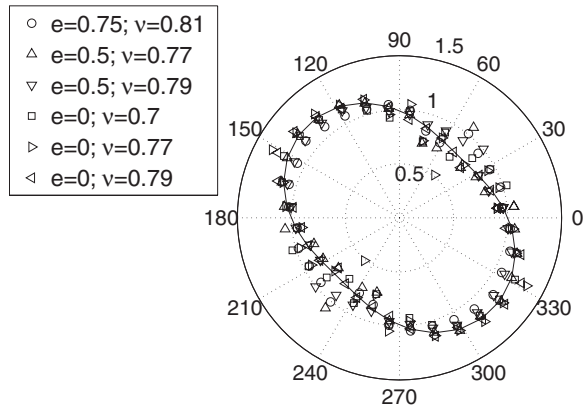
FIG. 9. Normalized angular dependence of the length scale, $\xi(\theta)/\xi$, for frictionless shear flows with different restitution coefficients and packing fractions. The data are well characterized by Eq. (4), plotted as a line.

axis due to a higher number of grain interactions, and destroyed along the dilational axis due to contacts being lost.

We note that the maximum value of the correlation length occurs at approximately the same angle for each packing fraction in Fig. 8. This trend is followed for other packing fractions and restitution coefficients as well. In Fig. 9 we plot the angular dependence of the length scale divided by its average value: $\xi(\theta)/\xi$. This collapses the data for a large range of packing fractions and restitution coefficients onto one curve. The collapse is not perfect, especially along the dilational axis of the shear flow where the correlations are small.

The common collapsed curve for all of the data in Fig. 9 demonstrates that ξ is anisotropic. The angular dependence of ξ can be approximated as a Fourier series, including only terms that are π periodic. We find that, as is the case for other anisotropies in granular flow [67–72], the functional form of $\xi(\theta)$ is well characterized by the first two terms in the Fourier series,

$$\xi(\theta) = \frac{\xi}{2\pi}[1 - a_0 \sin 2(\theta - \theta_0)], \qquad (4)$$

where ξ is the average value of the correlation length. The solid curve in Fig. 9 is a fit to this equation, which estimates the parameter values as $a_0 = 0.21$ and $\theta_0 = 0.013$. The value of θ_0 is consistent with the axis of maximum compression for the data we have gathered. This implies that larger values of ξ occur near $\theta = 3\pi/4$ because the compression induced by the shear flow causes more grains to come into contact. Near $\theta = \pi/4$, where ξ is a minimum, dilation reduces the magnitude of correlations and thereby the length scale. However, we have found no simple explanation for the value of a_0. We suspect that the numerical value of a_0 should be related to the anisotropy in the contact distribution [70]. However, because the anisotropy in ξ remains constant over a range of packing fractions and restitution coefficients, where the anisotropy in the contact distribution is not constant, the value of a_0 may have a simpler origin.

In this section we have measured spatial correlations between the total force on grains separated by a distance ℓ in two dimensions. In three dimensions, we expect the results to be qualitatively similar. This is because, in all dimensions, jamming occurs at a finite packing fraction ν_c and correlations must exist that span the system. The onset of correlations and their extent will surely depend on dimension, but for given values of e and μ there is a packing fraction $\nu_{bc} < \nu_c$ where correlations become significant. For $\nu > \nu_{bc}$ we expect the extent of the correlations to increase continuously and diverge at ν_c, analogously to the data we have presented for two-dimensional systems.
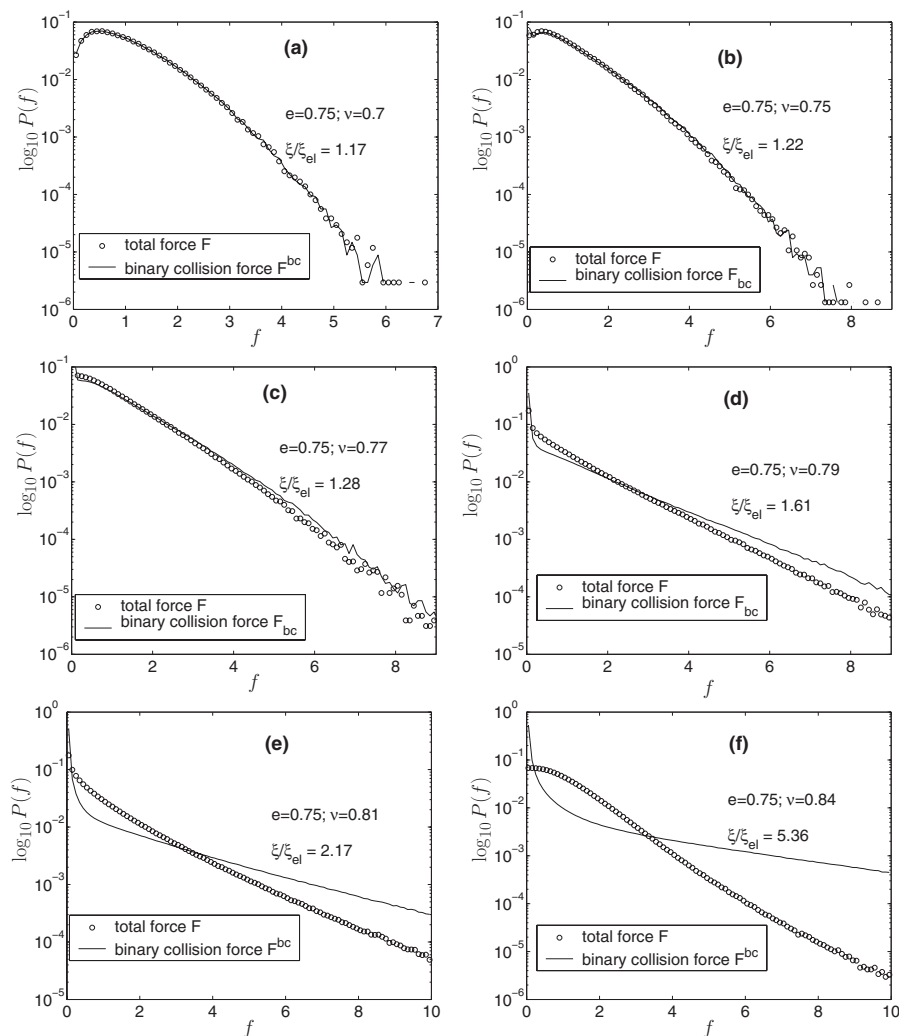
V. THE EFFECTS OF CORRELATIONS ON CONTACT FORCES

In the previous section we presented measurements of a correlation length ξ that diverges at the jamming transition and asymptotes to an elastic value ξ_{el} at small packing fraction. This length scale captures the decay of force correlations and is related to the emergence of clusters of simultaneously contacting grains. In very dilute systems only binary collisions are relevant, $\xi = \xi_{el}$, and contact forces can be determined from the properties of the two colliding grains. However, as the packing fraction is increased, ξ also increases, and the contact force between any two grains will depend on the properties of the other grains in the cluster. This is because, in the rigid grain limit, forces propagate instantaneously through the network. Because the growth of ξ is closely related to the nature of the force transfer—binary collisions or force networks—we expect the contact forces to depend on the value of ξ. A useful way to explore properties of contact forces is to measure the contact force probability distribution function (PDF) $P(F)$. This function encodes the statistics of the contact forces: $P(F)dF$ is proportional to the number of contact forces in the range from F to $F+dF$.

To make the connection between contact forces and spatial force correlations explicit, we begin by demonstrating that the contact forces between pairs of grains cannot be determined simply by assuming binary collisions when ξ is large. To illustrate this point, we compare the statistics of the actual contact forces to the forces we would calculate if we assumed that only binary collisions occurred. If we make the binary collision assumption, then the dynamical rule in Eq. (1), along with momentum conservation, determines the normal impulse in each collision. Dividing this impulse by the algorithm time step yields the average force that would arise over the time step dt. We label this force F_{bc}^{ij}, where i and j represent the colliding grains and the label "bc" reminds us that this force applies only to purely binary collisions. It is simple to show that the value of the binary force is given by

$$F_{bc}^{ij} = (1 + e)\mu^{ij}[(\mathbf{v}'^j - \mathbf{v}'^i) \cdot \hat{\boldsymbol{\sigma}}^{ij}]/dt, \qquad (5)$$

where e is the normal restitution coefficient, $\mu = m^i m^j/(m^i + m^j)$ is the reduced mass, $\mathbf{v}'^i$ is the precollisional velocity of grain i, and $\hat{\boldsymbol{\sigma}}^{ij}$ is the unit vector connecting the centers of grains i and j. All of these terms can be measured directly from simulations.

FIG. 10. $P(f)$ for systems with $e=0.75$ and increasing values of ξ/ξ_{el}, where f is the contact force F divided by the average value $\langle F \rangle$ (symbols). These data are compared with the line, where the force is determined from Eq. (5), which assumes that only binary collisions occur. We have normalized both the total forces and binary collision forces in each plot by their average values. There is excellent agreement for $\xi/\xi_{el} < 1.25$. For larger values of the correlation length, clusters of interacting grains form and the binary collision assumption does not fit the data.
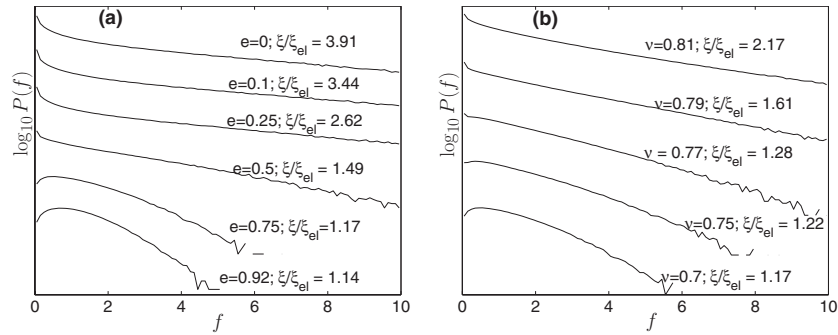
In Fig. 10 we plot measurements of the contact force distribution function $P(F)$ for $e=0.75$ and six increasing values of the packing fraction ν. In each figure, we compare $P(F)$ with the statistics of the binary forces $P(F_{bc})$. If these two functions are the same then contact forces are well approximated by considering only binary collisions; if the functions differ then we know that clusters of contacting grains affect contact forces.

We indicate the value of ξ/ξ_{el} for each plot in Fig. 10 and immediately see that for small values of ξ/ξ_{el} the data for $P(F)$ are well fitted by the line, which is a measurement of $P(F_{bc})$. However, as ξ increases, the presence of force networks changes the nature of the contact forces and we can no longer make accurate predictions by assuming that only binary collisions occur. The transition occurs between the values of $\xi/\xi_{el}=1.22$ and 1.28. Therefore $\xi/\xi_{el}=1.25\pm0.03$ serves as an upper bound for the regime where the binary collision assumption is reasonable. This value of ξ/ξ_{el} signals the transition between collisional and noncollisional flows for all restitution coefficients and packing fractions we have investigated.

In cases when $\xi/\xi_{el}>1.25$, force networks have formed and simultaneous contacts produce measurable effects on the forces between grains. In order to calculate the force between

two grains, it is not sufficient to consider only the properties of the two contacting grains; rather, all of the grains connected in the force network play an important role. This is because the two contacting grains are being pushed together by the other grains in the cluster and the contact force is equal to the binary collision contribution from Eq. (5) plus a contribution from the cluster.

The value $\xi/\xi_{el}=1.25\pm0.03$ separates the regime where only binary collisions occur from the regime where force networks begin to form and affect contact forces. This is the value of the length scale at which there is a clear deviation between binary collisional forces and total forces. Measurements presented later in this paper, and in the following paper [20], also place the network transition within these bounds. Although this value of the length scale does not change with restitution coefficient or friction, we would expect it to depend on the grain size distribution.

The techniques we used to determine the crossover in Fig. 10 can only be applied in simulations where the position, velocity, and force on every grain are always known. However, we have also found a signature of the transition that can be (and has been) observed in experiments of granular flows. This signature relates to the small force behavior of the contact force distribution function.

FIG. 11. Measurements of the contact force probability distribution function $P(f)$, where f is the value of the contact force divided by the average contact force. The different curves have been offset so that it is easy to see the qualitative changes in the functional form. (a) Data for $\nu = 0.7$ and different values of the restitution coefficient e. (b) Data for $e = 0.75$ and increasing values of the packing fraction ν. The curves in each plot are also labeled by their associated value of ξ/ξ_{el}, and we observe that the peak is present in $P(f)$ only if $\xi/\xi_{el} < 1.28$.

In Fig. 11 we present data for the contact force distribution function $P(F)$. In particular, we plot $\log_{10} P(f)$ for many different values of the restitution coefficient and packing fraction, where f is equal to the normal contact force F divided by the average normal force $\langle F \rangle$. All of these curves correspond to frictionless materials, but we have observed that the statistics of the normal forces display the same behavior for frictional systems. Our measurements of $P(f)$ have been averaged over 5000 time steps in steady state shear flow, and the different curves are vertically displaced in the figure so each can be clearly seen. Each curve is labeled by the value of ξ/ξ_{el} and we immediately see that the behavior at small f depends on the value of ξ. For $\xi/\xi_{el} \lesssim 1.25$ there is a clear peak, whereas for $\xi/\xi_{el} \gtrsim 1.25$ the peak disappears and the maximum occurs at $f = 0$.

This measurement once again defines a crossover around $\xi/\xi_{el} = 1.25$. This is the transition where the microscopic interactions change from being dominated by binary collisions between grains to being dominated by clusters of grains, forming force networks of size ξ/ξ_{el}. When this network transition occurs, the peak disappears and the most likely force is no longer equal to the average force. This is because grains have formed into transient clusters and the greatest number of contacts are simply rolling over each other, which produces a very small normal force. This moves the peak to $f = 0$ once the transition has fully developed and the average force is not representative of most of the forces. Additionally, as force networks become long ranged, the data show that there is a greater probability of large forces, which arise from a large number of grains in a cluster compressing two contacting grains.

We have also taken data for $P(F)$ close to the network transition point for granular flows with $e = 0.75$. In Fig. 12 we plot the value of the force F_{max} for which $P(F_{max})$ is a maximum, as a function of packing fraction. Between packing fractions of 0.766 and 0.767, our data show that the value of f_{max} (equal to F_{max} divided by the average force $\langle F \rangle$) makes a jump from approximately 0.2 to zero. Within this small range of packing fraction, the contact force PDF loses its peak. The abruptness of the transition suggests that different physical processes are occurring on either side of the transition and that the network transition is quite sharp.

The signature of the transition evident in our measurements of $P(f)$ has also been observed in other simulations and experiments, but has never been connected to the formation of large-scale structure. Simulations of granular hopper flow [73,74], conducted using event-driven simulations where only binary collisions are allowed to occur, have reported that, as the hopper aperture is reduced and the density of the packing increases, $P(f)$ begins to lose its peak. This is consistent with our results from Fig. 11 and suggests that the correlation length ξ is relevant in more than just shear flows of granular media. Additionally, the same behavior in $P(f)$ has been observed in experiments on hopper flow [47], which lends credibility to the result and suggests that it is not an artifact of the simulation methods used here and in Refs [73,74], but rather a real effect in granular flows.

The results we have cited from hopper flow, and others [75], have been used to challenge the belief that the formation of a peak in $P(f)$ is a signature of the jamming transition [76,79]. In a wide variety of contexts, including incline flow [76], quasistatic flow [22,77], and jammed granular materials [31–33,78], it has been observed that $P(f)$ exhibits a maximum at $f = 0$ (no peak) if the system is flowing, while a peak
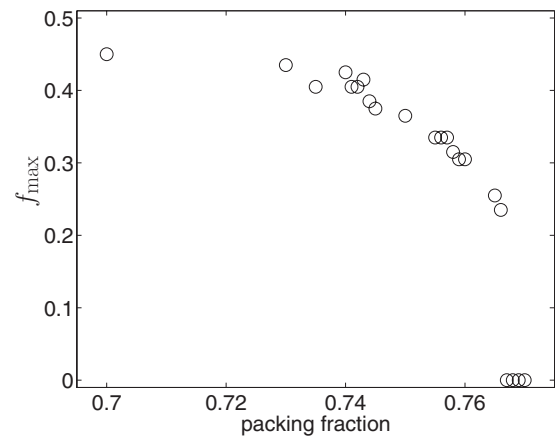

FIG. 12. Value f_{max} at which the contact force PDF $P(f_{max})$ is a maximum, as a function of packing fraction, for $e = 0.75$. The maximum of $P(f)$ occurs at positive f for $\nu \leq 0.766$ and at $f = 0$ for $\nu \geq 0.767$.

at nonzero f forms as the systems jams. These observations, coupled with similar results in Lennard-Jones glasses and foams [79], have been used to bolster the claim that the formation of a peak in $P(f)$ is a generic characteristic of the jamming transition, and a necessary condition for the appearance of a yield stress.

Our observations reveal that, in fact, there are two important transitions encoded in the small-f behavior of $P(f)$. First, at a low packing fraction, there is the network transition where interactions between grains change from binary collisions to force networks. This occurs in the inertial flow regime and is accompanied by a change in $P(f)$ where the peak that was present for small densities disappears and the maximum value of $P(f)$ occurs at $f=0$. Then, as shown elsewhere, there is another transition at higher packing fraction where the system develops a yield stress and the peak reappears in $P(f)$.

In summary, we have measured contact force distributions in this section to determine the effects of spatial force correlations. We find that $\xi/\xi_{el}=1.25$ separates the regime where only binary collisions occur from the regime where force networks form. This observation allows us to split the inertial regime where hard-sphere granular flows exist into two distinct regions. At low packing fraction there is a "dilute regime" where binary collisions are the dominant microscopic interaction and $\xi/\xi_{el}<1.25$. At high packing fraction there is a "dense regime" where force networks exist but do not percolate through the system. This dense regime is characterized by clusters of interacting grains with an average extent ξ/ξ_{el} in the range of $1.25<\xi/\xi_{el}<\infty$. For dilute flows where only binary collisions occur, a peak is visible in $P(f)$; as force networks begin to appear in the dense regime, the peak disappears.

The crossover at $\xi/\xi_{el}=1.25$ defines the transition between interactions dominated by binary collisions and interactions dominated by force networks. Therefore, we use this value to define $\nu_{bc}(e)$, which is the value of the packing fraction below which only binary collisions are relevant (shown schematically in Fig. 1). This function is plotted in Fig. 13 using the data for ξ from Fig. 4. This plot is for frictionless materials $\mu=0$, but increasing the value of μ does not change the curve. This is because, as we saw in Fig. 7, the effects of friction do not take hold until ξ is much larger than $1.25\xi_{bc}$. Thus ν_{bc} is an important packing fraction for all values of friction, and we see that it is an increasing function of e. This is because larger e produces less energy dissipation and restricts grain clustering. The data in Fig. 13 imply that as $e \rightarrow 1$ then $\nu_{bc} \rightarrow \nu_c \approx 0.845$, which is the packing fraction at which the system jams. This means that, as grains become perfectly elastic and no energy is dissipated at contacts, then binary collisions describe the interactions for all values of packing fraction before jamming.

VI. CONCLUSIONS

We have measured correlations between grain forces in inertial shear flows. These correlations decay exponentially with a characteristic length scale ξ that diverges at the jamming transition and asymptotes to an elastic value ξ_{el} in the
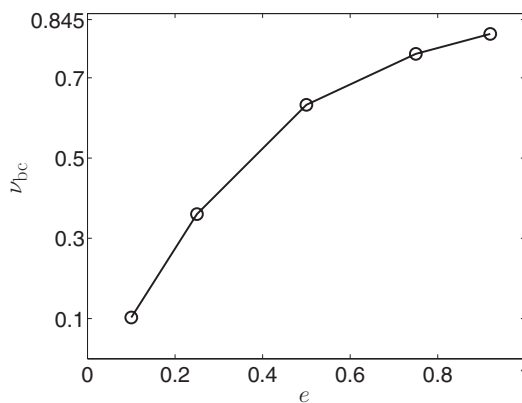

FIG. 13. Value of ν_{bc} as a function of restitution coefficient e. Below $\nu_{bc}(e)$ only binary collisions are relevant and above ν_{bc} force networks emerge. As e approaches unity, the network transition is concurrent with the jamming transition at $\nu_c \approx 0.845$.

dilute limit. By investigating the statistics of contact forces between grains, we have shown that $\xi/\xi_{el}=1.25$ splits the inertial regime into dilute flows, where all forces arise from binary collisions between grains, and dense flows, where force chain networks begin to form. We denoted by ν_{bc} the packing fraction at which $\xi/\xi_{el}=1.25$ and found that the value of ν_{bc} depends on the restitution coefficient, but is always less than the packing fraction ν_c at which the system jams. This phenomenology is illustrated in Fig. 14.

The crossover from the dilute to the dense regime is accompanied by a qualitative change in the nature of contact forces between grains, measured using the contact force dis-
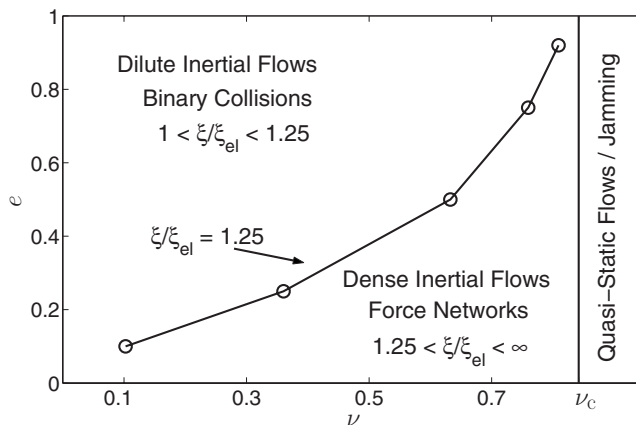

FIG. 14. State diagram of granular shear flow, plotted as a function of the packing fraction ν and the restitution coefficient e. For our system, we estimate that $\nu_c \approx 0.845$, which is represented by the vertical line on the plot. The value of ν_c separates the inertial regime from the quasistatic regime. In this paper we have focused on the inertial regime and shown that there is an important packing fraction ν_{bc} where $\xi/\xi_{el}=1.25$. Our measured values of ν_{bc} depend on the restitution coefficient and are plotted on the diagram. For $\nu < \nu_{bc}$ the flow is in the dilute inertial regime, where microscopic interactions consist of binary collisions; for $\nu > \nu_{bc}$ the flow is in the dense inertial regime where long-ranged force networks begin to form.

tribution function $P(f)$. For shear flows in the dilute regime $P(f)$ has a peak at nonzero f, whereas for shear flows in the dense regime there is no peak. This raises interesting questions about the nature of the transition that occurs at ν_{bc}. We observe that the average coordination number z is equal to 1 for flows with $\nu < \nu_{bc}$ and is greater than 1 for $\nu > \nu_{bc}$. Further investigation of the scaling behavior of granular flows very close to ν_{bc} is needed to bring further insight to the physics near the transition.

From a wider viewpoint, the presence of spatial correlations changes the assumptions that can be made when mod-

eling properties of the system. We explore the theoretical implications of correlations in the following paper [20].

ACKNOWLEDGMENTS

[1] H. M. Jaeger, S. R. Nagel, and R. P. Behringer, Rev. Mod. Phys. **68**, 1259 (1996).

[2] J. Feda, *Mechanics of Particulate Materials: The Principles* (Elsevier, Amsterdam, 1982).

[3] R. M. Nedderman, *Statics and Kinematics of Granular Materials* (Cambridge University Press, Cambridge, U.K., 1992).

[4] L. P. Kadanoff, Rev. Mod. Phys. **71**, 435 (1999).

[5] R. Albert, I. Albert, D. Hornbaker, P. Schiffer, and A.-L. Barabasi, Phys. Rev. E **56**, R6271 (1997).

[6] N. Fraysse, H. Thorne, and L. Petit, Eur. Phys. J. B **11**, 615 (1999).

[7] K. M. Frye and C. Marone, J. Geophys. Res. **107**, 2309 (2002).

[8] P. Tegzes, T. Vicsek, and P. Schiffer, Phys. Rev. E **67**, 051303 (2003).

[9] R. Brewster, G. S. Grest, J. W. Landry, and A. J. Levine, Phys. Rev. E **72**, 061301 (2005).

[10] K. Mair, K. M. Frye, and C. Marone, J. Geophys. Res. **107**, 2219 (2002).

[11] J. F. Wambaugh, C. Reichhardt, and C. J. Olson, Phys. Rev. E **65**, 031308 (2002).

[12] J. L. Anthony and C. Marone, J. Geophys. Res. **110**, B08409 (2005).

[13] J. A. Astrom and H. J. Herrmann, Eur. Phys. J. B **5**, 551 (1998).

[14] P. Cundall and O. D. L. Strack, Geotechnique **29**, 47 (1979).

[15] C. S. Campbell, Annu. Rev. Fluid Mech. **22**, 57 (1990).

[16] I. Goldhirsch, Annu. Rev. Fluid Mech. **35**, 267 (2003).

[17] A. Kudrolli, M. Wolpert, and J. P. Gollub, Phys. Rev. Lett. **78**, 1383 (1997).

[18] D. Bonamy, F. Daviaud, L. Laurent, M. Bonetti, and J. P. Bouchaud, Phys. Rev. Lett. **89**, 034301 (2002).

[19] D. L. Blair and A. Kudrolli, Phys. Rev. E **67**, 041301 (2003).

[20] G. Lois, A. Lemaitre, and J. M. Carlson, following paper, Phys. Rev. E **76**, 021303 (2007).

[21] P. Dantu, in *Proceedings of the Fourth International Conference on Soil Mechanics and Foundations Engineering* (Butterworths Scientific Publications, London, 1957).

[22] F. Radjai, M. Jean, J.-J. Moreau, and S. Roux, Phys. Rev. Lett. **77**, 274 (1996).

[23] T. S. Majmudar and R. P. Behringer, Nature (London) **435**, 1079 (2005).

[24] S. N. Coppersmith, C.-h. Liu, S. Majumdar, O. Narayan, and T. A. Witten, Phys. Rev. E **53**, 4673 (1996).

[25] J. E. S. Socolar, Phys. Rev. E **57**, 3204 (1998).

[26] P. Claudin, J.-P. Bouchaud, M. E. Cates, and J. P. Wittmer, Phys. Rev. E **57**, 4441 (1998).

[27] M. Nicodemi, Phys. Rev. Lett. **80**, 1340 (1998).

[28] J. E. S. Socolar, D. G. Schaeffer, and P. Claudin, Eur. Phys. J. E **7**, 353 (2002).

[29] M. Otto, J.-P. Bouchaud, P. Claudin, and J. E. S. Socolar, Phys. Rev. E **67**, 031302 (2003).

[30] J.-P. Bouchaud, P. Claudin, D. Levine, and M. Otto, Eur. Phys. J. E **4**, 451 (2001).

[31] D. M. Mueth, H. M. Jaeger, and S. R. Nagel, Phys. Rev. E **57**, 3164 (1998).

[32] G. Lovoll, K. J. Maloy, and E. G. Flekkoy, Phys. Rev. E **60**, 5872 (1999).

[33] L. E. Silbert, G. S. Grest, and J. W. Landry, Phys. Rev. E **66**, 061303 (2002).

[34] G. Frenning and G. Alderborn, Phys. Rev. E **71**, 011305 (2005).

[35] E. Aharonov and D. Sparks, Phys. Rev. E **60**, 6890 (1999).

[36] C. S. O'Hern, L. E. Silbert, A. J. Liu, and S. R. Nagel, Phys. Rev. E **68**, 011306 (2003).

[37] H. P. Zhang and H. A. Makse, Phys. Rev. E **72**, 011301 (2005).

[38] C. S. Campbell, J. Fluid Mech. **465**, 261 (2002).

[39] R. P. Behringer, D. Howell, L. Kondic, S. Tennakoon, and C. Veje, Physica D **133**, 1 (1999).

[40] D. M. Mueth, G. F. Debregeas, G. S. Karczmar, P. J. Eng, S. R. Nagel, and H. M. Jaeger, Nature (London) **406**, 385 (2000).

[41] L. E. Silbert, D. Ertas, G. S. Grest, T. C. Halsey, D. Levine, and S. J. Plimpton, Phys. Rev. E **64**, 051302 (2001).

[42] F. da Cruz, S. Emam, M. Prochnow, J.-N. Roux, and F. Chevoir, Phys. Rev. E **72**, 021309 (2005).

[43] W. R. Ketterhagen, J. S. Curtis, and C. R. Wassgren, Phys. Rev. E **71**, 061307 (2005).

[44] A. Lemaître, Phys. Rev. Lett. **89**, 064303 (2002).

[45] G. Lois, A. Lemaitre, and J. M. Carlson, Phys. Rev. E **72**, 051303 (2005).

[46] R. A. Bagnold, Proc. R. Soc. London, Ser. A **255**, 49 (1954).

[47] E. Longhi, N. Easwar, and N. Menon, Phys. Rev. Lett. **89**, 045501 (2002).

[48] J. J. Moreau, in *Nonsmooth Mechanics and Application: Courses and Lectures*, edited by J. J. Moreau and P. D. Panagiotopoulos (Springer-Verlag, Vienna, 1988), pp. 1–82.

[49] M. Jean and J.-J. Moreau, in *Proceedings of Contact Mechanics International Symposium* (Presses Polytechniques et Universitaires Romandes, Lausanne, Switzerland, 1992),

pp. 31–48.

[50] J. J. Moreau, in *Powders and Grains*, edited by C. Thornton (Brookfield, Rotterdam, The Netherlands, 1993), pp. 227–232.

[51] J. J. Moreau, Eur. J. Mech. A/Solids **13**, 93 (1994).

[52] D. E. Wolf, in *Computational Physics*, edited by K. H. Hoffmann and M. Schreiber (Springer, Berlin, 1996).

[53] M. Jean, Comput. Methods Appl. Mech. Eng. **177**, 235 (1999).

[54] S. F. Foerster, M. Y. Louge, H. Chang, and K. Allia, Phys. Fluids **6**, 1108 (1994).

[55] A. W. Lees and S. F. Edwards, J. Phys.: Condens. Matter **5**, 1921 (1972).

[56] D. J. Evans and G. P. Morriss, Phys. Rev. A **30**, 1528 (1984).

[57] M. Alam and C. M. Hrenya, Phys. Rev. E **63**, 061308 (2001).

[58] I. Goldhirsch and G. Zanetti, Phys. Rev. Lett. **70**, 1619 (1993).

[59] S. McNamara and W. R. Young, Phys. Rev. E **53**, 5089 (1996).

[60] G. Lois, A. Lemaitre, and J. M. Carlson, Europhys. Lett. **76**, 318 (2006).

[61] A. J. Liu and S. R. Nagel, Nature (London) **396**, 21 (1998).

[62] C. Moukarzel, P. M. Duxbury, and P. L. Leath, Phys. Rev. Lett. **78**, 1480 (1997).

[63] C. Moukarzel and P. M. Duxbury, Phys. Rev. E **59**, 2614 (1999).

[64] D. Ertas and T. C. Halsey, Europhys. Lett. **60**, 931 (2002).

[65] O. Pouliquen, Phys. Rev. Lett. **93**, 248001 (2004).

[66] O. Baran, D. Ertas, T. C. Halsey, G. S. Grest, and J. B. Lechman, Phys. Rev. E **74**, 051302 (2006).

[67] C. Thornton and D. J. Barnes, Acta Mech. **64**, 45 (1986).

[68] J. R. F. Arthur, J. A. Koenders, and R. K. S. Wong, Acta Mech. **64**, 19 (1986).

[69] L. Rothenburg and R. J. Bathurst, Geotechnique **39**, 601 (1989).

[70] F. Radjai, D. E. Wolf, M. Jean, and J.-J. Moreau, Phys. Rev. Lett. **80**, 61 (1998).

[71] N. P. Kruyt, Int. J. Solids Struct. **40**, 3537 (2003).

[72] H. Troadec, F. Radjai, S. Roux, and J. C. Charmet, Phys. Rev. E **66**, 041305 (2002).

[73] C. Denniston and H. Li, Phys. Rev. E **59**, 3289 (1999).

[74] A. Ferguson, B. Fisher, and B. Chakraborty, Europhys. Lett. **66**, 277 (2004).

[75] J. W. Landry and G. S. Grest, e-print arXiv:cond-mat/0506110.

[76] L. E. Silbert, D. Ertas, G. S. Grest, T. C. Halsey, and D. Levine, Phys. Rev. E **65**, 051307 (2002).

[77] F. Radjai, S. Roux, and J.-J. Moreau, Chaos **9**, 544 (1999).

[78] J. W. Landry, G. S. Grest, L. E. Silbert, and S. J. Plimpton, Phys. Rev. E **67**, 041303 (2003).

[79] C. S. O'Hern, S. A. Langer, A. J. Liu, and S. R. Nagel, Phys. Rev. Lett. **86**, 111 (2001).